

The extended X-ray emission around RRAT J1819–1458

A. Camero–Arranz¹, N. Rea¹, M.A. McLaughlin², N. Bucciantini^{3,4},
P. Slane⁵, B. Gaensler⁶, D. Torres^{1,7}, L. Stella⁸, E. de Oña¹,
G. Israel⁸, F. Camilo^{9,10} and A. Possenti¹¹

¹Institut de Ciències de l'Espai, (IEEC-CSIC), Campus UAB, Fac. de Ciències,
Torre C5-parell, 2a planta, 08193 Barcelona, Spain
email: camero@ice.cat

²Department of Physics, West Virginia University, Morgantown, WV 26501, USA

³INAF - Osservatorio Astrofisico di Arcetri, L.go E. Fermi 5, 50125, Firenze, Italy

⁴INFN - Sezione di Firenze, Via G. Sansone 1, 50019 Sesto Fiorentino, Firenze, Italy

⁵Harvard-Smithsonian Center for Astrophysics, 60 Garden St. Cambridge, MA 02138, USA

⁶The University of Sydney, Room 216, 44 Rosehill Street, Redfern, NSW 2016, Australia

⁷Institució Catalana de Recerca i Estudis Avancats (ICREA)

⁸INAF - Osservatorio Astronomico di Roma, Via Frascati 33, Roma, Italy

⁹Columbia Astrophysics Lab, Columbia University, New York, NY 10027, USA

¹⁰Arecibo Observatory, HC3 Box 53995, Arecibo, PR 00612, USA

¹¹INAF-Osservatorio Astronomico di Cagliari, 09012 Capoterra, Italy

Abstract. We present new imaging and spectral analysis of the recently discovered extended X-ray emission around the high-magnetic-field rotating radio transient RRAT J1819–1458. We used two *Chandra* observations, taken on 2008 May 31 and 2011 May 28. The diffuse X-ray emission was detected with a significance of $\sim 19\sigma$ in the image obtained by combining the two observations. Long-term spectral variability has not been observed. Possible scenarios for the origin of this diffuse X-ray emission, further detailed in Camero–Arranz *et al.* (2012), are here discussed.

Keywords. pulsars: individual (RRAT J1819–1458) — stars: magnetic fields — stars: neutron — X-rays: stars

1. Introduction

Rotating Radio Transients (RRATs) are radio pulsars that were discovered through their sporadic radio bursts (McLaughlin *et al.* 2006). At a radio frequency of 1.4 GHz, radio bursts are observed from RRAT J1819–1458 roughly every ~ 3 minutes with the Parkes telescope. The spin period of RRAT J1819–1458 is 4.3 s, with a characteristic age of 117 kyr at a 3.6 kpc distance and a dipolar magnetic field of $B \sim 5 \times 10^{13}$ G. The spin-down energy loss rate measured for this source is $\dot{E}_{rot} \sim 3 \times 10^{32}$ erg s⁻¹, being the only source of this type also detected in X-rays (Reynolds *et al.* 2006, McLaughlin *et al.* 2007, Rea *et al.* 2008, Kaplan *et al.* 2009). In this work, we present the study of the extended X-ray emission discovered by Rea *et al.* (2009), resulting from the reduction and combined analysis of two *Chandra* observations for RRAT J1819–1458, performed on 2008 and 2011 May 28.

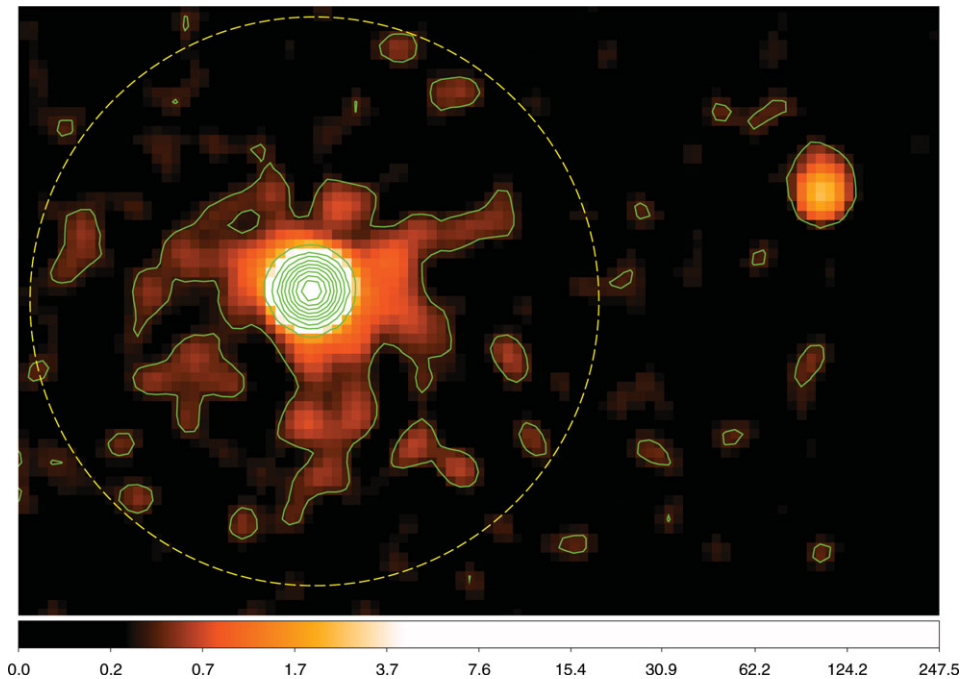


Figure 1. Combined 0.3–10 keV log image of RRAT J1819–1458, with a circular region of 15'' overlotted and the 3σ contours of the extended emission (Camero-Arranz *et al.* 2012). One ACIS-S pixel is $0''.492$.

2. Observations and data reduction

The *Chandra* X-ray Observatory observed RRAT J1819–1458 with the Advanced CCD Imaging Spectrometer (ACIS) instrument on 2008 May 31 (ObsID 7645) for 30 ks and again in 2011 May 28 (ObsID 12670) for 90 ks, both in VERY FAINT (VF) timed exposure imaging mode. For both observations, we used a 1/8 subarray, which provides a time resolution of 0.4 s. Standard processing of the data using CIAO software (ver. 4.4) has been performed.

3. Analysis and results

3.1. Imaging

To study the extended X-ray emission found by Rea *et al.* (2009) in more detail, we proceeded with the extraction of a combined image in the 0.3–10 keV energy range, using the two *Chandra* observations using the CIAO tool `reproject_image`. Figure 1 shows the resultant combined image where diffuse extended X-ray emission is clearly visible around the compact object. We applied the CIAO `wavdetect` tool to the ~ 90 ks ACIS-S cleaned image and found RRAT J1819–1458 at the following position: $\alpha = 18^{\text{h}}19^{\text{m}}34.18^{\text{s}}$ and $\delta = -14^{\circ}58'03''.7$ (error circle of $0''.5$ radius), in agreement with previous results.

3.2. Spectroscopy

We used the CIAO `specextract` script to extract source and background spectra for RRAT J1819–1458. To increase the signal to noise of the spectrum we proceeded to combine the spectra created for ObsID 7645 and 12670 using the CIAO tool `combine_spectra` (see Figure 2). The combined spectrum was modeled with an absorbed blackbody plus an

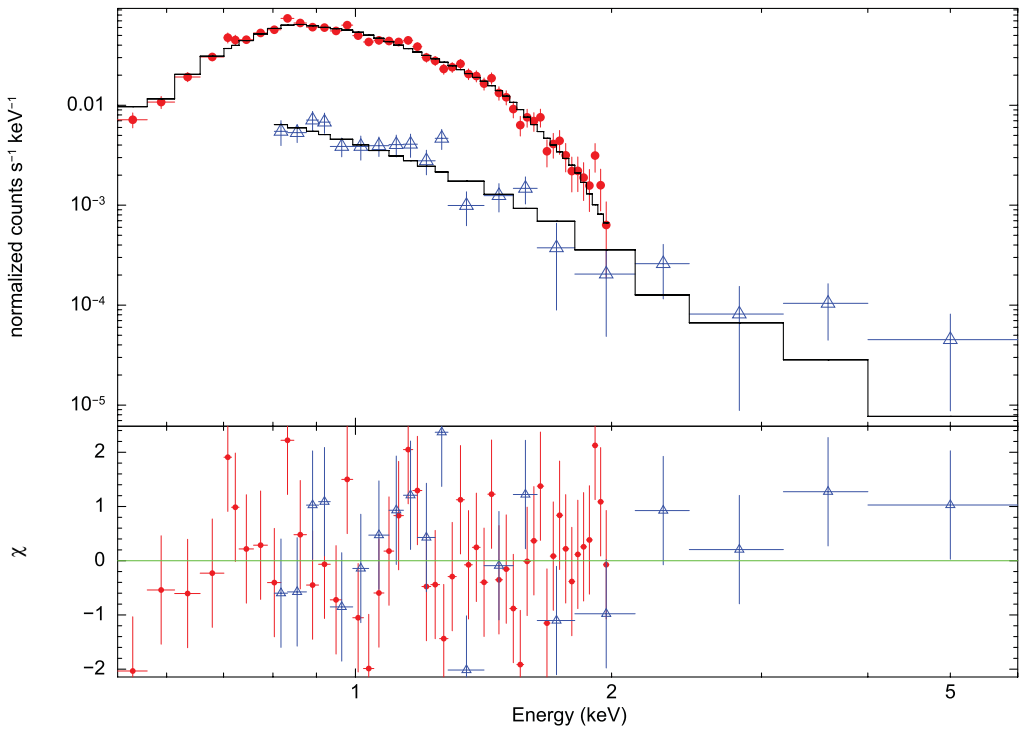


Figure 2. Red circles denote the combined ACIS-S spectrum of RRAT J1819–1458†. Blue open triangles represent the combined spectrum of the extended X-ray emission (Camero-Arranz *et al.* 2012).

absorption line at 1 keV. The Hydrogen absorption column was fixed to $0.6 \times 10^{22} \text{ cm}^{-2}$, allowing us to better constrain the 1 keV line feature. The blackbody temperature obtained was $T_{\text{Body}} = 0.130 \pm 0.002 \text{ keV}$, with $E_{\text{gauss}} = 1.16 \pm 0.03 \text{ keV}$ and $\sigma = 0.17 \pm 0.03 \text{ keV}$ ($\chi_r^2 = 1.10$; 44 dof). Figure 2 also shows the $\sim 0.8\text{--}7 \text{ keV}$ combined spectrum for the extended source. An absorbed power law provides a good fit to the data. The spectral parameters resulted from the best fitting are $\alpha = 3.7 \pm 0.3$ ($\chi_r^2 = 1.26$; 19 dof).

3.3. The diffuse X-ray emission structure

To infer the significance and estimate the luminosity of the whole diffuse emission in the combined image, we built the combined Chart/MARX point-spread function (PSF), using both the RRAT J1819–1458 spectrum and its corresponding exposure time. In Figure 3, we compare the surface brightness radial distribution of the combined Chandra observation of RRAT J1819–1458 with that of the combined Chart/MARX PSF plus a background level. This figure shows that the extended emission becomes detectable around 5 pixels ($\sim 2''.5$) from the peak of the source PSF. To compute the significance of the diffuse X-ray emission around RRAT J1819–1458, from the combined image we extracted all the photons from an annular region of $2''.5\text{--}20''$ radii, and we subtracted from it the background extracted from a similar region far from the source. This resulted in an excess of 790 ± 18 counts (a detection significance of $\sim 19\sigma$).

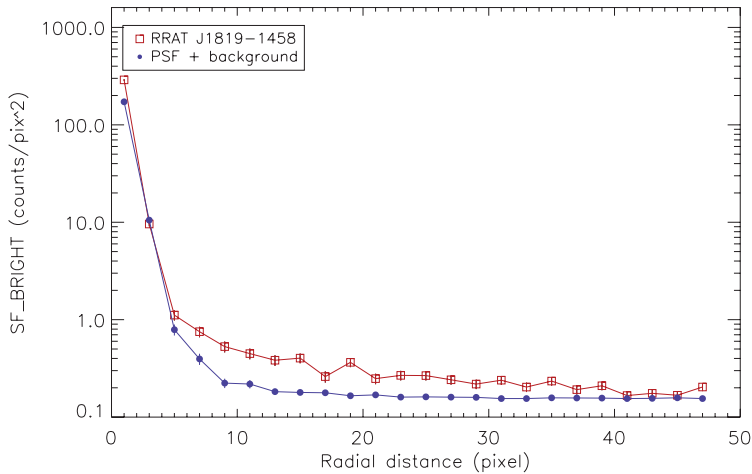


Figure 3. Surface brightness of the background-subtracted ACIS-S image of RRAT J1819–1458 shown in red open squares, and of the Chart/MARX PSF plus a constant background shown as blue circles (Camero-Arranz *et al.* 2012).

4. Discussion

The energies of pulsar wind electrons and positrons range from ~ 1 GeV to ~ 1 PeV, placing their synchrotron and inverse Compton emission into radio–X–ray and GeV–TeV bands, respectively. This multiwavelength emission can be seen as a pulsar-wind nebula. To date, the exact physical origin and acceleration mechanism of the high-energy particles in the pulsar winds are poorly understood, and not all nebulae can be easily explained as spin-down-powered PWNe. In Rea *et al.* (2009) we discussed different scenarios for the origin of the extended emission detected around RRAT J1819–1458. One option was that the extended emission we observe is part of the remnant of the supernova explosion which formed RRAT J1819–1458, unlikely for an object of 117 kyr. A bow-shock nebula due to the pulsar moving supersonically through the ambient medium was also ruled out due to the projected velocity in the case of a bow shock ($v_p \sim 20$ km s $^{-1}$; see Rea *et al.* 2009 and references therein) being rather small. We propose that RRAT J1819–1458 could power a sort of PWN or the extended X–ray emission around the pulsar might be explained as a magnetic nebula, or as a scattering halo as for 1E 1547–5408 (Vink & Bamba 2009, Olausen *et al.* 2011) and Swift J1834.9–0846 (Younes *et al.* 2012; Esposito *et al.* 2012).

References

- Camero-Arranz, A., Rea, N., Bucciantini, N. *et al.* 2012, *submitted to MNRAS*
 Esposito, P., Tiengo, A., Rea, N. *et al.* 2012, *submitted to MNRAS*
 Kaplan, D. L., Esposito, P., Chatterjee, S., *et al.* 2009, *MNRAS* 400, 1445
 Lyne, A. G., McLaughlin, M. A., Keane, E. F. *et al.* 2009, *MNRAS* 400, 1439
 McLaughlin, M. A., Lyne, A. G., Lorimer, D. R. *et al.* 2006, *Nature* 439, 817
 McLaughlin, M. A., Rea, N., Gaensler, B. M. *et al.* 2007, *ApJ* 670, 1307
 Olausen, S. A., Kaspi, V. M., Ng, C.-Y. *et al.* 2011, *ApJ*, 739, 94
 Rea, N. & McLaughlin, M. 2008, in Yuan, Y.-F. and Li, X.-D. and Lai, D. (eds.), *American Institute of Physics Conference Series*, Vol. 968, pp 151–158
 Rea, N., McLaughlin, M. A., Gaensler, B. M. *et al.* 2009, *ApJ* 703, L41
 Reynolds, S. P., Borkowski, K. J., Gaensler, B. M., Rea, N. *et al.* 2006, *ApJ* 639, L71
 Vink, J., Bamba, A., & Yamazaki, R.: 2011, *ApJ* 727, 131
 Younes, G., Kouveliotou, C., Kargaltsev, O. *et al.* 2012, *ApJ*, *in press*, arXiv:1206.3330